

Bayesian analysis of five open clusters in the Milky Way

M.S. Pera¹, G.I. Perren¹, G. Carraro⁴, E. Giorgi¹, H.D. Navone² & R.A. Vázquez¹

¹ *Facultad de Ciencias Astronómicas y Geofísicas (UNLP), Instituto de Astrofísica de La Plata (IALP-CONICET), La Plata, Argentina.*

² *Facultad de Ciencias Exactas, Ingeniería y Agrimensura (FCEIA-UNR), Instituto de Física de Rosario (IFIR-CONICET).*

³ *Dipartimento di Fisica Astronomia Galileo Galilei, Vicolo Osservatorio 3, Padova, Italy*

Contact / msolpera@gmail.com

Resumen / Presentamos resultados derivados de la aplicación de nuestra herramienta Automated Stellar Cluster Analysis (ASteCA) sobre cinco cúmulos abiertos mayormente ignorados, ubicados en el Tercer Cuadrante de la Vía Láctea. Nuestra fotometría *UBV* Johnson-Kron-Cousin fue combinada con datos de la segunda publicación de datos de la misión Gaia. Obtenemos probabilidades de membresía y finalmente se utiliza un algoritmo Bayesiano MCMC para derivar los parámetros fundamentales de los cúmulos.

Abstract / We present results derived from the application of our Automated Stellar Cluster Analysis (ASteCA) tool on five mostly overlooked open clusters, located in the Third Quadrant of the Milky Way. Our *UBV* Johnson-Kron-Cousin photometry was combined with data from the second data release of the Gaia survey. Membership probabilities are obtained and finally a Bayesian MCMC algorithm is used to derive the clusters' fundamental parameters.

Keywords / Methods: statistical – Galaxies: star clusters: general – (Galaxy:) open clusters and associations: general – Techniques: photometric– Parallaxes – Proper motions

1. Introduction

The five clusters analyzed in this article are: Ruprecht 41, Ruprecht 42, Ruprecht 44, Ruprecht 152, and Haffner 14 (RUP41, RUP42, RUP44, RUP152, HAF14). These are all mostly overlooked open clusters located in the Third Quadrant of the Milky Way. We cross-matched our *UBV* Johnson-Kron-Cousin photometry, obtained using the 1.0 m Swope telescope* at Las Campanas, Chile, with publicly available data from the second data release of the Gaia survey (DR2). This allows us to add the *G* magnitude along with parallax and proper motions data, to our full set of observed stars.

ASteCA (Perren et al., 2015) is a powerful tool especially developed to perform an automatic analysis of observational cluster data (structural, photometric, and if available, parallax and proper motions). A comprehensive study of stellar coordinates allows the code to determine center and cluster radius values. Following this, membership probabilities are assigned to all stars within the defined cluster regions through a Bayesian decontamination algorithm. This method combines photometric data with parallax and proper motions to better estimate the per-star probability of being a cluster member. Finally, a (parallel-tempered) Bayesian Markov Chain Monte Carlo (MCMC) algorithm is applied to derive the fundamental parameters: metallicities, ages, extinctions, distances, and masses.

2. Analysis

The analyzed frames for two of the five clusters (RUP44 and HAF14) are shown in Fig. 1 as examples, as given by the DSS colored survey. Center coordinates for all clusters are shown in Table 1. The analyzed data is composed of *UBV* photometry cross-matched with Gaia DR2 parallaxes and proper motions. A small fraction of the processes applied by ASteCA on the data associated to each cluster are presented in Figs. 2, 3 and 4. The parallax data from Gaia DR2 is shifted by an offset of +0.029 mas, as suggested by Lindegren et al. (2018). More recent studies suggest that this offset might be too conservative, and larger values (up to +0.075 mas) have been suggested.

Table 1: Center coordinates for each cluster

Name	RA (2000)	DEC (2000)
RUP 41	07:53:51.81	-26:57:42.9
RUP42	07:57:38.88	-25:56:6.0
RUP44	07:58:54.00	-28:34:60.0
RUP152	07:54:30.48	-38:13:12.0
HAF14	07:44:49.20	-28:22:48.0

The structural density maps for RUP44 and HAF14 are shown in Fig. 2. This analysis is performed to help identify the center coordinates, and the radius used to limit the cluster region (green lines and green circle, respectively). About half of the clusters are immersed

*<https://obs.carnegiescience.edu/swope>

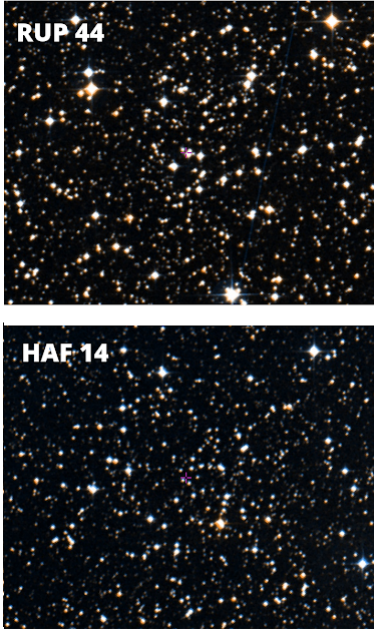


Figure 1: Frames for two of the five open clusters analyzed, located in the Third Quadrant of the Milky Way. Images obtained through the Aladin (CDS) service.

in regions of heavy field stars contamination, as can be seen in the density maps.

A Bayesian decontamination algorithm is applied over all the stars within this cluster region, to assign membership probabilities to all of them. This algorithm compares the color - magnitude (CMD) position of observed stars within the cluster region, with those of field stars in the same CMD. In this case we employ the V vs $(B - V)$ vs $(U - B)$ three dimensional CMD to perform this analysis. The colors in Fig. 3 and Fig. 4 for the plotted stars (ie: those within the cluster region) are associated to these probabilities.

In Fig. 3 we show the Bayesian parallax analysis proposed by Bailer-Jones (2015) on the cluster region stars. This analysis makes use of all stars, even those with negative parallax values of no apparent (physical) value. The distances obtained are heavily affected by the selected offset applied on the parallax, so they should be taken with care.

To estimate the clusters' fundamental parameters, i.e.: metallicity, age, extinction, distance, and total mass, AStECA generates synthetic clusters that are compared to the observed one. This analysis is performed millions of times with the aim of estimating each parameter's probability distribution. To this end, we employed a Bayesian MCMC algorithm. The algorithm is called `ptemcee` (Vousden et al., 2016) and it is used to explore the posterior probability of all the free parameters involved in the model. Only the binary fraction parameter is fixed to 0.3, which is a commonly accepted value for open clusters (Sollima et al., 2010). In Fig. 4 we show the result of applying this analysis

Table 2: Results obtained for the metallicity ($[\text{Fe}/\text{H}]$), age ($\log(\text{age})$), extinction (E_{BV}), distance modulus (dm), and mass (M in solar masses) of all the cluster. Mean values and standard deviations (in parenthesis, below) are shown.

Name	$[\text{Fe}/\text{H}]$	$\log(\text{age})$	E_{BV}	dm	M
RUP41	0.16 (0.10)	8.63 (0.20)	0.28 (0.02)	13.71 (0.14)	200 (100)
RUP42	-0.25 (0.16)	8.34 (0.05)	0.39 (0.01)	14.01 (0.06)	800 (200)
RUP44	-0.22 (0.09)	7.21 (0.02)	0.69 (0.01)	13.33 (0.06)	700 (100)
RUP152	-0.63 (0.27)	8.58 (0.02)	0.59 (0.01)	14.76 (0.11)	1800 (100)
HAF14	-1.05 (0.38)	8.66 (0.03)	0.66 (0.01)	12.23 (0.05)	1100 (100)

method to our cluster sample.

All clusters are younger than 500 million years, with metal content values that range from markedly sub-solar like HAF14, to slightly above solar in the case of RUP41. RUP44 is affected by the largest extinction, reaching almost the maximum value estimated by

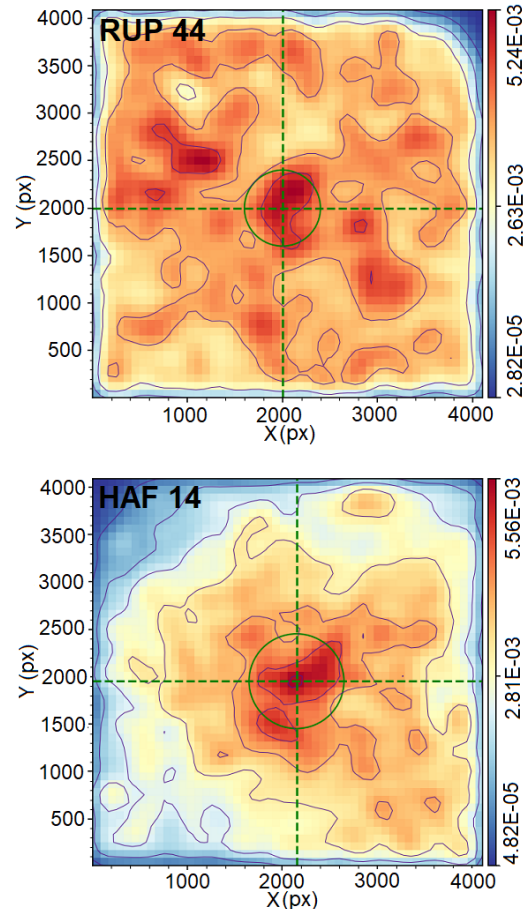


Figure 2: Structural density maps for two of the five clusters: RUP44, HAF14. The color bars to the right are associated with the stellar density in the field.

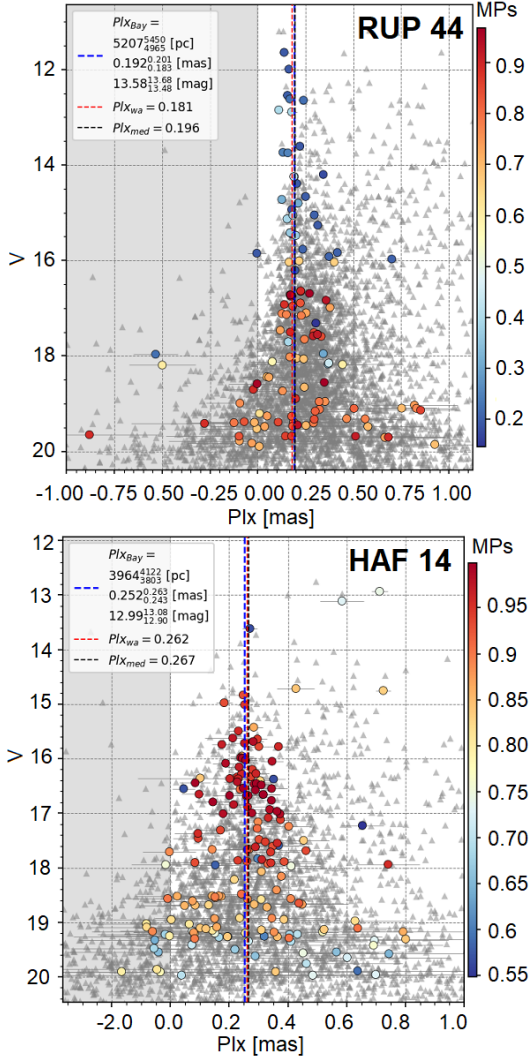


Figure 3: Bayesian parallax analysis for two of the five clusters. The dashed vertical lines represent: Bayesian distance obtained (blue), weighted average of the parallaxes (red), median of the parallaxes (black). The colorbars to the right indicate membership probability values.

Schlafly & Finkbeiner (2011) of ~ 0.7 mag. It is also the youngest cluster in the sample.

Table 2 summarizes the results obtained for the fundamental parameters of all the studied clusters. There are appreciable differences in the distances estimated by Gaia parallax versus ASteCA’s photometric analysis. The difference between the Gaia and the ASteCA based estimates are: RUP41 ≈ -1.5 kpc, RUP42 ≈ -0.8 kpc, RUP44 ≈ 0.6 kpc, HAF14 ≈ 1.2 kpc, RUP152 ≈ -1.8 kpc.

3. Conclusions

The results of applying ASteCA over the combined UB+G (Johnson-Kron-Cousin plus Gaia systems) photometric data are very promising. The Bayesian inference method recently included in the code is able to

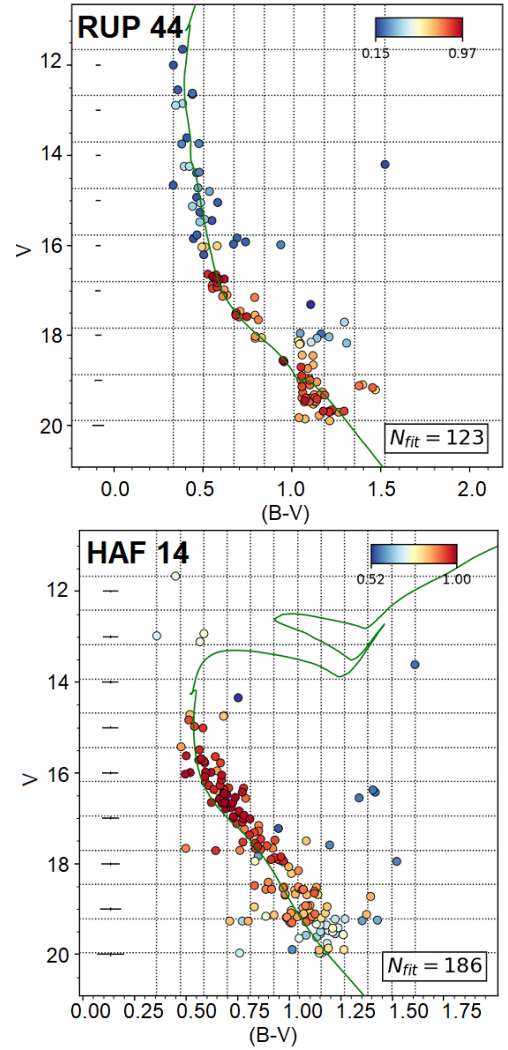


Figure 4: Two of the five observed clusters (RUP44, HAF14) and the isochrone (in green) used to generate final best fit synthetic cluster N_{fit} indicates the number of stars used in the fitting process.

find very reasonable solutions for all the cluster’s parameters explored, as shown in Table 2. We expect to further develop this method in upcoming versions of ASteCA, particularly aiming at improving its performance.

References

- Bailer-Jones C.A.L., 2015, PASP, 127, 994
- Lindgren L., et al., 2018, A&A, 616, A2
- Perren G.L., Vázquez R.A., Piatti A.E., 2015, A&A, 576, A6
- Schlafly E.F., Finkbeiner D.P., 2011, ApJ, 737, 103
- Sollima A., et al., 2010, MNRAS, 401, 577
- Vousden W.D., Farr W.M., Mandel I., 2016, MNRAS, 455, 1919